Cell

Small-Molecule Inhibition of the Interaction between the Translation Initiation Factors eIF4E and eIF4G

Nathan J. Moerke,[1] Huseyin Aktas,[2] Han Chen,[2] Sonia Cantel,[2] Mikhail Y. Reibarkh,[1] Amr Fahmy,[1] John D. Gross,[1,4] Alexei Degterev,[3,5] Junying Yuan,[3] Michael Chorev,[2] Jose A. Halperin,[2] and Gerhard Wagner[1,*]
[1] Department of Biological Chemistry and Molecular Pharmacology, Harvard Medical School, Boston, MA 02115, USA
[2] Laboratory for Translational Research, Harvard Medical School, One Kendall Square, Building 600, 3rd Floor, Cambridge, MA 02139, USA
[3] Department of Cell Biology, Harvard Medical School, Boston, MA 02115, USA
[4] Present address: Department of Pharmaceutical Chemistry, University of California, San Francisco, 600 16th Street, S-512E, Box 2280, San Francisco, CA 94143, USA.
[5] Present address: Department of Biochemistry, Tufts University School of Medicine, 136 Harrison Avenue, Stearns 703C, Boston, MA 02111, USA.
*Correspondence: gerhard_wagner@hms.harvard.edu
DOI 10.1016/j.cell.2006.11.046

SUMMARY

Assembly of the eIF4E/eIF4G complex has a central role in the regulation of gene expression at the level of translation initiation. This complex is regulated by the 4E-BPs, which compete with eIF4G for binding to eIF4E and which have tumor-suppressor activity. To pharmacologically mimic 4E-BP function we developed a high-throughput screening assay for identifying small-molecule inhibitors of the eIF4E/eIF4G interaction. The most potent compound identified, 4EGI-1, binds eIF4E, disrupts eIF4E/eIF4G association, and inhibits cap-dependent translation but not initiation factor-independent translation. While 4EGI-1 displaces eIF4G from eIF4E, it effectively enhances 4E-BP1 association both in vitro and in cells. 4EGI-1 inhibits cellular expression of oncogenic proteins encoded by weak mRNAs, exhibits activity against multiple cancer cell lines, and appears to have a preferential effect on transformed versus nontransformed cells. The identification of this compound provides a new tool for studying translational control and establishes a possible new strategy for cancer therapy.

INTRODUCTION

The regulation of gene expression at the level of translation initiation is critical for proper control of cellular growth, proliferation, differentiation, and apoptosis. In eukaryotes a set of initiation factors (eIFs) are required to dissociate the 40S and 60S ribosomal subunits, to recruit the mRNA and initiator tRNA to the 40S subunit, and to promote joining of the 60S subunit so that elongation can commence (Dever, 2002; Hershey and Merrick, 2000). The major rate-limiting step in initiation is thought to be localization of the small ribosomal subunit to the 5′ end of the mRNA. This process requires the stepwise assembly of a large multiprotein complex centered on the trimer eIF4F. eIF4F is composed of the cap-binding protein eIF4E, the RNA helicase eIF4A, and the multidomain adaptor protein eIF4G (Gingras et al., 1999; von der Haar et al., 2004). Cap-bound eIF4F recruits the 40S ribosomal subunit through the eIF3/eIF4G interaction, which initiates scanning to the initiation codon, where the 40S subunit joins with the 60S subunit. This process is facilitated by eIF4A, with the requirement for its helicase activity directly proportional to the amount of secondary structure in the 5′ untranslated region (UTR) that must be melted for scanning to occur (Svitkin et al., 2001). All eIF4G proteins bind eIF4E through a motif of sequence $Y(X)_4L\Phi$, where X is variable and Φ is hydrophobic (Altmann et al., 1997; Mader et al., 1995). This motif forms a helical peptide structure that binds to a conserved surface of hydrophobic residues on the dorsal side of eIF4E (Marcotrigiano et al., 1999). In *Saccharomyces cerivisiae* this motif is part of a larger folded domain that forms an extended binding interface with eIF4E (Gross et al., 2003; Hershey et al., 1999), but it is unclear whether a larger interface exists in higher eukaryotes. Although the $Y(X)_4L\Phi$ motif may not be sufficient for full affinity binding of mammalian eIF4G to eIF4E, the fact that mutations in this sequence can abrogate binding indicates that it is necessary for this protein-protein interaction (Mader et al., 1995).

Cellular mRNAs differ greatly in the amount of eIF4F they require for efficient translation and in the composition of their 5′ UTRs. The majority of growth- and proliferation-related proteins are encoded by "weak" mRNAs containing long, highly structured 5′ UTRs that have lower

translational efficiency than "strong" mRNAs, which contain relatively short and unstructured 5′ UTRs (Lodish, 1976; Pickering and Willis, 2005). Translation of weak mRNAs is highly eIF4F dependent and is preferentially enhanced when the eIF4F complex level is increased by eIF4E overexpression (Koromilas et al., 1992). The amount of eIF4F in the cell is normally controlled by a class of small proteins termed 4E-BPs (Pause et al., 1994) that sequester eIF4E from eIF4G (Haghighat et al., 1995; Richter and Sonenberg, 2005). These proteins contain the $Y(X)_4L\Phi$ sequence found in eIF4G, and, using this motif, they can bind with high affinity to the same surface of eIF4E (Marcotrigiano et al., 1999). The activity of 4E-BPs is regulated by hierarchical phosphorylation at a set of conserved serine and threonine residues: hyperphosphorylated forms bind much more weakly than hypophosphorylated forms, and they are released from eIF4E (Gingras et al., 2001). The kinase mTOR is the major upstream regulator of 4E-BPs: stimuli such as nutrients and growth factors induce 4E-BP phosphorylation and increased cellular eIF4F through signaling pathways that activate mTOR (Averous and Proud, 2006; Mamane et al., 2006; Petroulakis et al., 2006; Tee and Blenis, 2005; Wullschleger et al., 2006).

Misregulation of cap-dependent translation plays an important role in human disease. A number of genetic disorders characterized by aberrant cell growth, such as hypertrophic cardiopathy and tuberous sclerosis, are caused by mutations that disregulate the mTOR pathway (Inoki et al., 2005; Lee et al., 2006). Abnormal amounts of cellular eIF4F caused by elevated levels of initiation factors or misregulation of 4E-BP phosphorylation can play a key role in tumorigenesis (Bjornsti and Houghton, 2004; De Benedetti and Graff, 2004; Petroulakis et al., 2006). Overexpression of eIF4E (Avdulov et al., 2004; Lazaris-Karatzas et al., 1990) or eIF4G (Fukuchi-Shimogori et al., 1997) can induce malignant transformation in mammalian cells. Conversely, ectopic expression of 4E-BPs can partially revert eIF4E-transformed cells to a nonmalignant phenotype (Rousseau et al., 1996) and induce apoptosis in cells transformed by other oncogenes such as Ras (Avdulov et al., 2004; Li et al., 2002). Peptides containing the $Y(X)_4L\Phi$ motif also can induce apoptosis in mammalian cells (Herbert et al., 2000). In transgenic mouse models, eIF4E overexpression promotes tumorigenesis (Ruggero et al., 2004; Wendel et al., 2004), while 4E-BP1 expression suppresses it (Polunovsky et al., 2000). This is consistent with the finding that, in humans, a variety of tumor types exhibit elevated levels of eIF4E (Ruggero and Pandolfi, 2003). Thus, the eIF4F complex is considered to be an important target for cancer therapy. RNA that is antisense to eIF4E has been shown to suppress the oncogenic properties of a head and neck carcinoma cell line (DeFatta et al., 2000). In addition, several analogs of rapamycin, a drug that decreases eIF4F levels by inhibiting mTOR-dependent 4E-BP phosphorylation, have antitumor activity and are being evaluated as cancer drugs in clinical trials (Bjornsti and Houghton, 2004; Faivre et al., 2006; Huang and Houghton, 2003; Sawyers, 2003).

Chemical genetics is a powerful tool for the study of cellular processes. High-throughput screens of compound libraries have been successfully used to identify new small-molecule modulators of translation initiation (Bordeleau et al., 2005, 2006; Novac et al., 2004). An increasingly important strategy in chemical genetics is the identification of compounds that disrupt specific protein-protein interactions (Arkin and Wells, 2004). Such inhibitors potentially offer a highly selective way to modulate the function of protein complexes and in many cases have therapeutic potential. Extended protein-protein interfaces typically contain "hot spots," which are compact regions of conserved residues that are critical for binding affinity and that are attractive targets for the development of small-molecule inhibitors. In the eIF4E/eIF4G interface the group of conserved eIF4E surface residues that contact the $Y(X)_4L\Phi$ peptide constitute such a site. We reasoned that small molecules that compete with this peptide for binding to eIF4E would inhibit the eIF4E/eIF4G interaction.

RESULTS AND DISCUSSION

Development of Fluorescence Polarization Assay

In order to identify compounds that disrupt the interaction between eIF4E and the $Y(X)_4L\Phi$ motif of eIF4G, we have developed a high-throughput fluorescence polarization (FP)-binding assay. A peptide containing the sequence KYTYDELFQLK was synthesized and tagged with fluorescein. Titration of this peptide with eIF4E causes the FP and the fluorescence anisotropy (FA) to increase almost 3-fold, and fitting the data into previously described equations (Roehrl et al., 2004) yields a peptide K_D of 3 μM (Figure 1A). As a positive control to validate the assay, the addition of an unlabeled competitor eIF4GII peptide (with the sequence KKQYDREFLLDFQFMPA) was shown to cause the FP to return to the level of free labeled peptide (Figure 1B). Fitting of this data for the unlabeled peptide yields an estimated K_D of 200 nM. This is close to the previously reported value of 150 nM, which was determined by isothermal titration calorimetry (Marcotrigiano et al., 1999). Thus, the principle of the screen is to identify the compounds that displace the labeled peptide from eIF4E by detecting the resulting decrease in FP. For the initial screen we used the 16,000 compound Chembridge DiverSet E library, from which a compound that we have termed 4EGI-1 (for eIF4E/eIF4G interaction inhibitor) was identified (Figure 1D). Analysis of the labeled peptide displacement caused by this compound as measured by FA (which is directly related to FP) shows the compound is a competitive inhibitor of eIF4G peptide binding (Figure 1C). In order to examine the specificity of 4EGI-1 we have synthesized two analogs, 4EGI-1A and 4EGI-N (Figure 1D). While 4EGI-N does not displace the labeled peptide, 4EGI-1A has activity similar to that of 4EGI-1 (Figure 1C). Fitting these data to a three-component (eIF4E, peptide, inhibitor) competition equilibrium yields, for eIF4E binding of 4EGI-1 and 4EGI-1A, K_D estimates

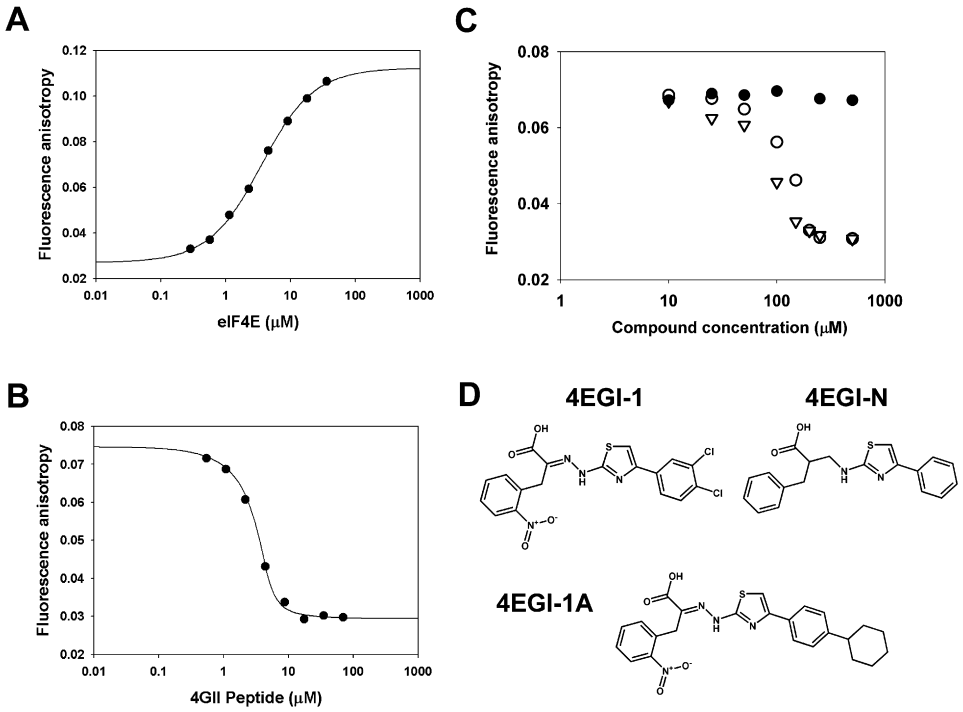

Figure 1. A FP Assay Identifies the Compound 4EGI-1 as a Competitive Inhibitor of the eIF4E/eIF4G Interaction

(A) Titration of a fluorescein-labeled eIF4G peptide with eIF4E causes increased FA. A best fit of the data to a two-state binding model is shown and yields an estimated K_D of 3 μM for binding of the labeled peptide to eIF4E.

(B) Competitive inhibition of labeled-peptide binding to eIF4E by an unlabeled eIF4GII peptide as measured by decrease in FA. A best fit of the data to a three-state binding model is shown and yields a K_D of 200 nM for the binding of the unlabeled peptide to eIF4E.

(C) Competitive inhibition of labeled-peptide binding to GB1-eIF4E by the compounds 4EGI-1 and 4EGI-1A. Full circles indicate 4EGI-N, empty circles indicate 4EGI-1, and triangles indicate 4EGI-1A.

(D) Structures of the compounds 4EGI-1, 4EGI-N, and 4EGI-1A.

of 25 μM ± 11 μM and 16 μM ± 6 μM, respectively. These values provide rough estimates (as the errors indicate) of the upper bound of the binding affinity for eIF4E. The fact that 4EGI-1 and 4EGI-1A exist in two interconverting isomeric forms in aqueous solution (see below) significantly complicates fitting the multiple binding equilibria involved and does not allow a more accurate determination of the K_Ds.

Characterization of 4EGI-1 Interaction with eIF4E by Nuclear Magnetic Resonance

Nuclear magnetic resonance (NMR) spectroscopy was used to characterize the interaction of 4EGI-1 with eIF4E. In order to confirm the direct binding of 4EGI-1 to eIF4E, we titrated this molecule with perdeuterated protein and monitored the ^{1}H-NMR spectrum of the compound. Titration of 4EGI-1 causes significant line broadening of resonances in the spectrum of the compound, which indicates binding to eIF4E (Figures 2A and S3). On the other hand, a similar titration with the inactive analog compound 4EGI-N shows little effect, which provides evidence that the binding of 4EGI-1 is not due to nonspecific hydrophobic interactions with the protein (Figure 2C). Examination of the ^{1}H-NMR spectrum of 4EGI-1 in aqueous solution shows that it can interconvert between the two isomers and that one of the isomers is preferentially bound by eIF4E. This does not allow a straightforward determination of a K_D (see above). Replacement of one nitrogen with a carbon (4EGI-N) eliminates this isomerization but also renders the compound inactive.

We next wished to determine by chemical shift mapping the location of 4EGI-1 interaction. Although chemical shift assignments have been reported for a complex of murine eIF4E with an eIF4G peptide (Miura et al., 2003), we needed to determine assignments for the free protein. Since mammalian eIF4E behaves poorly in solution, it was necessary to develop a more soluble form of the protein. To accomplish this, an N-terminal fusion of eIF4E to the 56 residue GB1 domain of protein G was constructed. This fusion domain has been shown to act as a solubility enhancement tag (SET) for heterologous proteins (Zhou et al., 2001). The GB1-eIF4E fusion has greatly enhanced solubility relative to that of native eIF4E. The presence of the GB1 domain does not affect the structure of eIF4E (Figure S1), and the fusion protein has the same binding affinity for the eIF4G peptide in the FP assay. Using this construct we obtained backbone chemical shift assignments for mammalian eIF4E. We proceeded to titrate

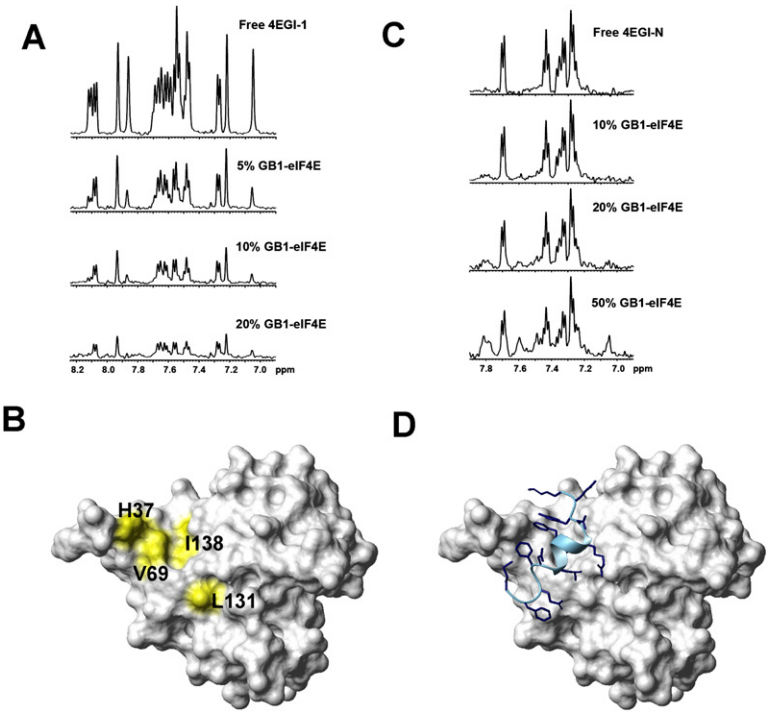

Figure 2. Characterization of the Interaction of 4EGI-1 with eIF4E by NMR

(A) ^{1}H-NMR spectra of 4EGI-1 measured at increasing concentrations of perdeuterated GB1-eIF4E indicate compound binding to eIF4E as determined by the decrease in intensity of peaks due to intermediate exchange broadening. The presence of two sets of signals indicates introconversion of two isomers, one of which binds preferentially to eIF4E, in aqueous solution.

(B) Location of residues on the eIF4G-binding surface of eIF4E with HSQC peaks that are preferentially broadened when titrated with 4EGI-1. The surface representation of the structure of eIF4E from the crystal structure of the eIF4E/eIF4GII peptide complex (Marcotrigiano et al., 1999) is shown with specific residues shaded in yellow. Image was generated using MOLMOL (Koradi et al., 1996).

(C) ^{1}H-NMR spectra of 4EGI-N measured at increasing concentrations of perdeuterated GB1-eIF4E indicate that the compound does not bind eIF4E. The presence of only one set of compound peaks indicates that this analog does not isomerize (due to the replacement of the central nitrogen with a carbon).

(D) Location of binding of the eIF4GII peptide. The same surface representation as (C) is shown from the same crystal structure with the peptide drawn in blue.

GB1-eIF4E with 4EGI-1 and to measure the effect on the ^{15}N-HSQC spectrum (Figure S2). While no effect on the GB1 resonances is observed, a set of the eIF4E peaks is attentuated due to line broadening. This indicates specific binding of the compound to eIF4E with intermediate exchange kinetics, which are typical of relatively tight ligand-protein interactions. Mapping the locations of the surface-exposed residues that are the most attenuated in intensity onto the structure of eIF4E (Figure 2B) shows that they cluster around the site of eIF4G peptide binding (Figure 2D). After extensive dialysis of fully titrated GB-eIF4E to remove any bound compound this line broadening disappears, which indicates that the binding of 4EGI-1 to eIF4E is reversible (data not shown).

4EGI-1 Disrupts the eIF4F Complex and Inhibits Cap-Dependent Translation In Vitro

We proceeded to characterize this compound in rabbit reticulocyte lysate, which is a well-established in vitro model system for studies of eukaryotic translation. To determine if 4EGI-1 can disrupt the eIF4F complex, the compound was incubated in rabbit reticulocyte lysate, and the state of association of eIF4E with eIF4G and 4E-BP1 was determined by pull-down on m^{7}GTP Sepharose resin (Figure 3A). This demonstrated that full-length eIF4G is displaced from eIF4E by 4EGI-1 in a dose-dependent manner. Surprisingly this compound does not inhibit binding of 4E-BP1 to eIF4E and instead causes a significant apparent increase in the amount of this protein that is bound. The increase in the level of eIF4E-bound 4E-BP1 is approximately 2- to 4-fold, as estimated by western blotting with purified 4E-BP1 as a concentration standard (data not shown). We speculate that this effect is likely due to the existence on eIF4E of a larger 4E-BP1 footprint that partially overlaps with that of eIF4G. A number of previous studies have provided strong evidence that this is the case. NMR chemical shift mapping of yeast eIF4E titrated with 4E-BP1 shows that there is a binding surface that is larger than just the area of residues that interact with the consensus peptide (Matsuo et al., 1997). Recently, it was found that full-length 4E-BP1 binds to eIF4E with significantly higher affinity than the consensus peptide alone (Tomoo et al., 2006). To confirm that 4EGI-1 does not inhibit binding of 4E-BP1 to eIF4E, we carried out a pull-down assay using purified eIF4E (without the GB1 tag) and 4E-BP1. Concentrations of 4EGI-1 that would be expected to bind a significant proportion of the available eIF4E do not cause any apparent decrease in 4E-BP1 binding (Figure 3B). Our data and the aforementioned studies support a model in which 4EGI-1 displaces eIF4G from eIF4E and clears the docking site for 4E-BP1, thus effectively increasing the amount of the protein bound to available eIF4E (Figure S4).

We then examined the effect of eIF4F complex disruption on translation in reticulocyte lysate using a dicistronic mRNA construct that encodes two luciferases (Figure 3C). The *Renilla* luciferase is translated in a cap-dependent fashion, while translation of firefly luciferase is driven by

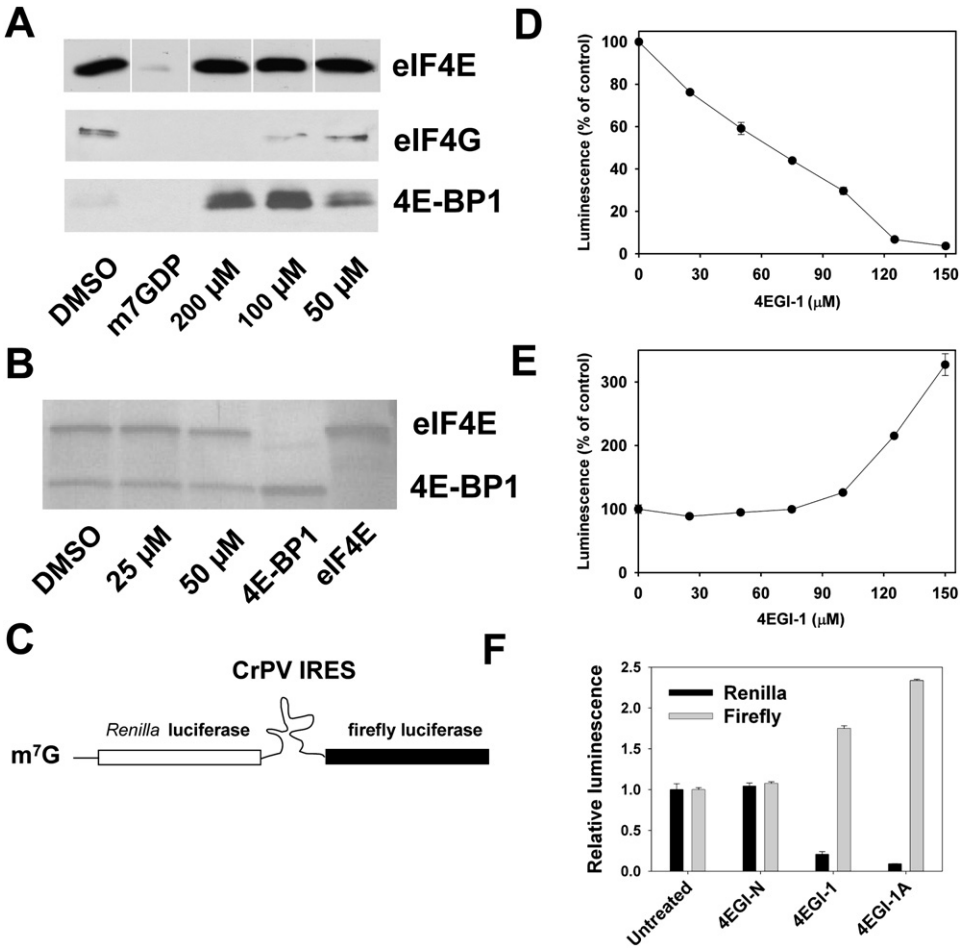

Figure 3. 4EGI-1 Disrupts eIF4F Complex Formation and Inhibits Cap-Dependent Translation

(A) 4EGI-1 displaces eIF4G from eIF4E and enhances 4E-BP1 binding in reticulocyte lysate. After incubation of aliquots of lysate with compound, cap-affinity chromatography and SDS-PAGE immunoblotting were used to detect eIF4E, eIF4G, and 4E-BP1. The eIF4E lanes shown come from the same gel and western blot.

(B) 4EGI-1 does not inhibit binding of purified 4E-BP1 to eIF4E. The two proteins were mixed in the presence of increasing compound concentrations and subjected to cap-affinity chromatography. Silver staining was used to detect bound proteins. Purified eIF4E and 4E-BP1 are included on the gel as molecular weight markers.

(C) Structure of a dual-luciferase mRNA reporter construct containing *Renilla* luciferase, the cricket paralysis virus IRES, and firefly luciferase.

(D) 4EGI-1 inhibits cap-dependent *Renilla* luciferase translation. *Renilla* luciferase activity was quantitated by measurement of luminescence and normalized relative to a DMSO-treated control reaction. Data points represent mean of triplicate measurements with error bars corresponding to standard error of the mean.

(E) 4EGI-1 does not inhibit firefly luciferase translation. Firefly luciferase activity was quantitated by measurement of luminescence and normalized relative to a DMSO-treated control reaction. Data points represent mean of triplicate measurements with error bars corresponding to standard error of the mean.

(F) Effects of 4EGI-1 and its analogs on translation are correlated with inhibition of eIF4G peptide binding to eIF4E. Translation of *Renilla* and firefly luciferases in reactions treated with 100 μM 4EGI-1, 4EGI-N, or 4EGI-1A was quantitated by luminescence measurements and was normalized to a control reaction containing an equivalent percentage of DMSO. Data points represent mean of duplicate measurements with error bars corresponding to standard error of the mean.

the cricket paralysis virus IRES, which is independent of initation factors (Pestova and Hellen, 2003). Cap-dependent translation is inhibited by 4EGI-1 (Figure 3D), while initiation factor-independent translation is not inhibited and instead is enhanced (presumably due to increased availability of ribosomes as cap-dependent translation is shut down; Figure 3E). The inactive analog 4EGI-N has no significant effect on cap-dependent or IRES-driven translation, while the active analog 4EGI-1A has an effect similar to that of 4EGI-1 (Figure 3F).

Next we examined the effect of 4EGI-1 on translation of the HCV and EMCV IRESs, both of which utilize translation-initiation factors. In rabbit reticulocyte lysate, 4EGI-1 can inhibit translation from the EMCV IRES at higher

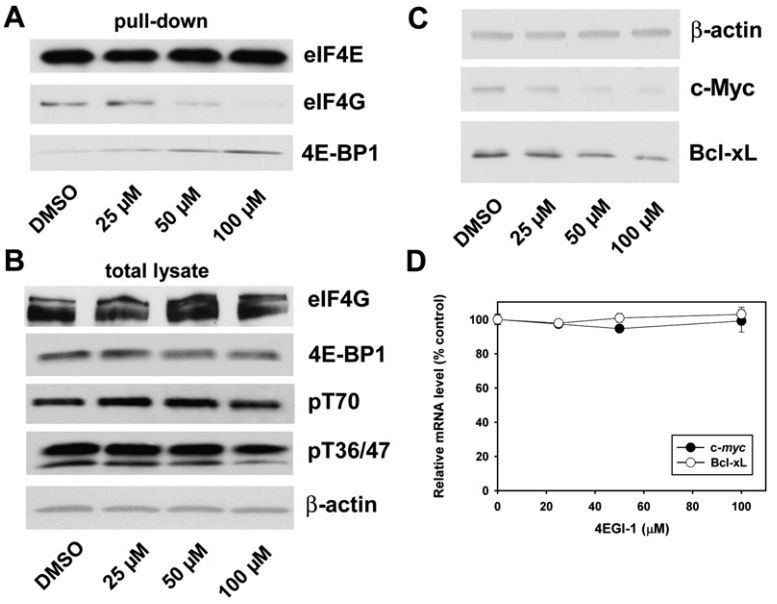

Figure 4. 4EGI-1 Disrupts the eIF4F Complex and Inhibits Expression of Oncogenic Proteins in Mammalian Cells

(A) 4EGI-1 displaces eIF4G from eIF4E and enhances 4E-BP1 binding in Jurkat cells. After 6 hr treatment with compound, extract preparation, cap-affinity chromatography, and SDS-PAGE immunoblotting were used to detect eIF4E, eIF4G, and 4E-BP1.

(B) Effect of 4EGI-1 on total eIF4G, 4E-BP1, and 4E-BP1 phosphorylation. After 6 hr treatment with compound, preparation of total cell extracts and SDS-PAGE immunoblotting were used to detect eIF4G, 4E-BP1, 4E-BP1 phosphorylated at T37/46, and 4E-BP1 phosphorylated at T70. An immunoblot for β-actin is shown as a control for total protein in the extract.

(C) 4EGI-1 downregulates expression of the c-Myc and Bcl-xL proteins. After 8 hr treatment with compound, preparation of total cell extracts and SDS-PAGE immunoblotting were used to detect β-actin, c-Myc, and Bcl-xL.

(D) 4EGI-1 does not affect the cytosolic levels of c-*myc* and Bcl-xL mRNAs. After 8 hr treatment with compound, preparation of cytosolic mRNA, and cDNA synthesis, the amount of mRNA relative to β-actin mRNA was quantitated by real-time PCR using the ΔΔCt method. Data points represent mean of triplicate measurements with error bars corresponding to standard error of the mean.

concentrations than needed to inhibit cap-dependent translation (Figure S5). One explanation for this could be that the efficiency of translation from the EMCV IRES is affected by the binding of eIF4E to eIF4G. Although this IRES does not directly require eIF4E, it does require eIF4G, and conformational changes in eIF4G caused by eIF4E binding may affect the efficiency of initiation from this IRES, at least in vitro. It is also possible that the compound has some "off-target" effects at the concentrations used in this study and inhibits the function of an additional factor or factors involved in EMCV IRES-driven translation. The HCV IRES is also inhibited by 4EGI-1 at a higher concentration than that needed to inhibit cap-dependent translation (Figure S5), which also could be due to "off–target" effects.

Activity of 4EGI-1 in Mammalian Cells

In order to determine if 4EGI-1 can disrupt the eIF4F complex in cells as well as in extracts we examined the effect of this compound on Jurkat leukemia T cells. Similar to the effect in vitro, compound treatment causes eIF4G to be displaced from eIF4E, while binding of 4E-BP1 is increased (Figure 4A). The total cellular levels of eIF4G and 4E-BP1 do not change significantly under these conditions, and there does not appear to be proteolytic cleavage of these proteins (Figure 4B). A possible alternative explanation for this result is that 4EGI-1 disrupts the pathways controlling phosphorylation of 4E-BP1. To test this possibility, we examined the cellular levels of phosphorylated forms of 4E-BP1 relative to total 4E-BP1 and found that they are not affected by the compound treatment (Figure 4B). This leads us to conclude that the displacement of eIF4G is due to binding of 4EGI-1 to eIF4E. Both in vitro and in cells, the estimated IC_{50} for displacement of eIF4G from eIF4E is similar to that for inhibition of cap-dependent translation (Table S1). The in vitro IC_{50} values for displacement of full-length eIF4G and for inhibition of cap-dependent translation are lower than that in the FP assay. This is presumably due to the lower level of eIF4E. We proceeded to examine the effect of 4EGI-1 on protein expression, hypothesizing that this compound would downregulate proteins encoded by weak mRNAs while having little effect on those encoded by strong mRNAs. In extracts of Jurkat cells treated with 4EGI-1, examination of protein levels by western blotting showed that the level of β-actin (which has a short, unstructured 5′ UTR) is unaffected, while expression of c-*myc* and Bcl-xL (both of which have long, highly structured 5′ UTRs) is signficantly decreased (Figure 4C). β-actin is a classic housekeeping protein and is encoded by a strong mRNA, while c-Myc and Bcl-xL are both oncogenic proteins encoded by weak mRNAs. To rule out the possibility of downregulated transcription or nucleocytosolic transport, cytosolic mRNA was prepared from treated cells, and quantitative real-time PCR was used to determine the effect of compound treatment on the levels of c-*myc* and Bcl-xL mRNAs. No significant change in mRNA level with increasing compound concentration was observed (Figure 4D).

Since regulation of cap-dependent translation plays an important role in cell survival, we wished to examine whether 4EGI-1 can induce apoptosis. Incubation of Jurkat cells with the compound induces cell death after 24 hr, as determined by measurement of the intracellular

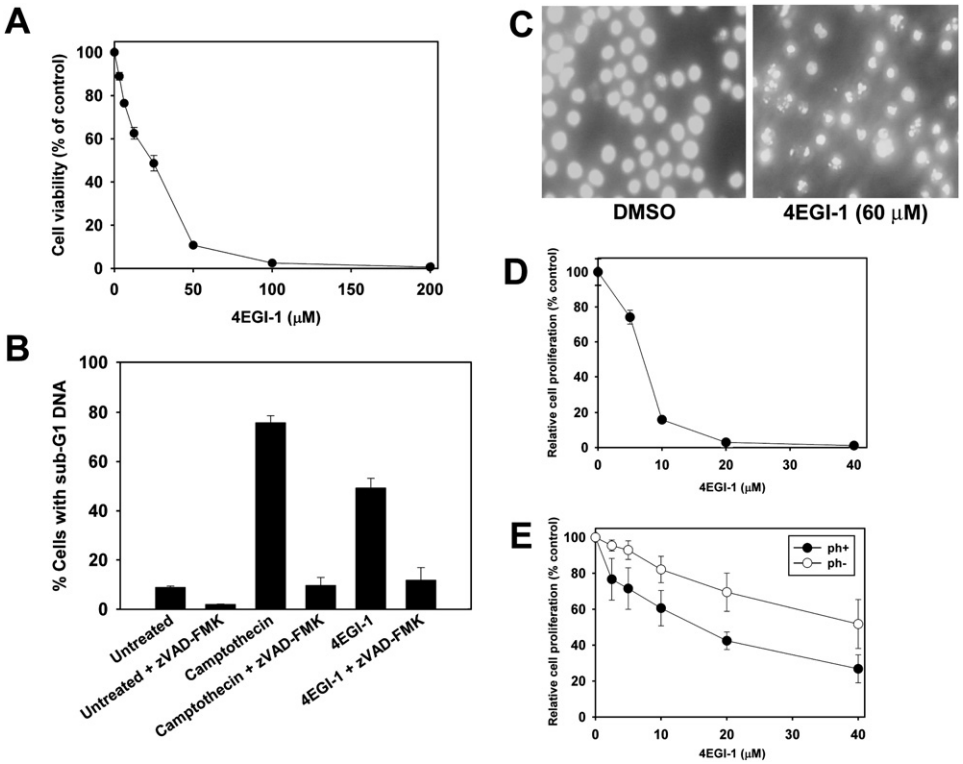

Figure 5. 4EGI-1 Has Proapoptotic Activity and Inhibits the Growth of Multiple Cancer Cell Lines

(A) 4EGI-1 treatment causes cell death in the Jurkat cell line. Twenty-four hours after addition of the compound, cell viability was quantitated by addition of CellTiter Glo reagent and by measurement of luminescence. Viability was normalized relative to DMSO-treated control cells. Data points represent mean of triplicate measurements with error bars corresponding to standard error of the mean.

(B) 4EGI-1 causes a significant increase in the cellular subG1 DNA content that is suppressed by cotreatment with zVAD-FMK. After 24 hr treatment with varying combinations of compounds, the percentage of total cells having a subG1 DNA content was determined by propidium iodide staining and by sorting in a FACS machine. Bars represent the mean of triplicate measurements with error bars corresponding to standard error of the mean.

(C) 4EGI-1 causes an apoptotic nuclear morphology. After 24 hr treatment with DMSO (control) or 60 μM 4EGI-1, cells were stained with Hoechst 33342 and visualized by fluorescence microscopy. Representative micrographs of control and treated cells are shown.

(D) 4EGI-1 treatment inhibits the proliferation of A549 lung cancer cells. Five days after cells were seeded at low density and compound was added, the level of cell proliferation was quantitated by SRB staining and by absorbance measurement. Proliferation was normalized relative to DMSO-treated control cells. Data points represent mean of triplicate measurements with error bars corresponding to standard error of the mean.

(E) 4EGI-1 treatment preferentially inhibits the growth of transformed pH+ cells but not nontransformed pH− cells. Three days after cells were seeded at low density and treated with compound, the level of cell growth was quantitated using a Beckman Coulter cell counter. Proliferation was normalized relative to DMSO-treated control cells. Data points represent mean of three independent experiments with error bars corresponding to standard error of the mean.

ATP level using a luminescent assay (Figure 5A). To find out if this cytotoxic activity is due to induction of apoptosis, we determined the ability of 4EGI-1 treatment to cause DNA fragmentation. Compound treatment causes a significant increase in subG1 DNA content in treated cells (Figure 5B); this is suppressed by cotreatment with the caspase inhibitor zVAD-FMK. In addition, the nuclei of treated cells have a fragmented morphology that is characteristic of apoptosis (Figure 5C). The demonstration that 4EGI-1 has proapoptotic activity in Jurkat cells suggested that this compound may exhibit activity against other cancer cell lines. The effect of this compound was tested using the NCI-SRB assay on A549 lung cancer cells (Figure 5D). This demonstrated that 4EGI-1 potently inhibits cell growth with an IC_{50} of approximately 6 μM. Because translation of weak mRNAs is highly sensitive to the level of eIF4F in the cell, it is likely that even small decreases in the level of this complex can cause a disproportionate biological effect in cells. This would explain why the observed IC_{50} values for apoptosis of Jurkat cells and the inhibition of A549 cell proliferation are lower than both the estimated affinity of 4EGI-1 for eIF4E and the IC_{50} for displacement of eIF4G from eIF4E (Table S1). One prediction that we made was that 4EGI-1 will have a stronger effect on transformed cells than on nontransformed cells due to the greater sensitivity of the former to inhibition of cap-dependent translation. To determine if this compound has a preferential effect on isogenic-transformed versus -nontransformed cells, we tested its effect on the growth of the Ph^+ cell line, which

is transformed by the *bcr-abl* oncogene. For comparison purposes we used Ph^- cells, which are from an isogenic cell line that is not transformed. Testing the effect of the compound on cell growth showed that 4EGI-1, with an IC_{50} for Ph^+ cells more than 2-fold lower than for Ph^- cells (Figure 5E), has a significantly more potent effect on transformed cells.

Conclusions

Our results demonstrate that it is possible to inhibit the protein-protein interaction between eIF4E and eIF4G using small molecules, and establish a methodology that can readily be used to identify new classes of such inhibitors through the screening of compound libraries. Major goals for future studies include a more detailed characterization of the mechanism of 4EGI class compounds in mammalian cells and a determination of how specific these compounds are for inhibition of eIF4E/eIF4G complex formation and for cap-dependent translation. This will be facilitated by synthesis of a larger set of analogs of 4EGI-1 for use in structure-activity studies. In addition, experimental modulation of eIF4E, eIF4G, and/or 4E-BP levels in cells treated with these compounds will aid in evaluating their specificity.

The observation that 4EGI-1 inhibits the binding of eIF4G, but not 4E-BP1, to eIF4E is somewhat unexpected and of particular interest. By shifting the equilbrium away from eIF4E/eIF4G complexes in favor of eIF4E/4E-BP1 complexes, 4EGI-1 appears to effectively enhance the activity of 4E-BP1. Although both eIF4G and 4E-BP1 contain the same $Y(X)_4L\Phi$-consensus motif, there is evidence that the binding footprint of 4E-BP1 may be larger and may involve contacts outside of this sequence. Up to this point attempts to determine the structure of the complex of eIF4E by using full-length 4E-BP1 (as opposed to smaller peptides) have not been successful due to the presence of extensive NMR line broadening in the complex and the failure of this complex to crystallize. It is possible that displacement of eIF4G from eIF4E by 4EGI-1 may free up the binding site for 4E-BP1 by removing steric obstruction. Future structural studies will reveal the molecular basis of the specificity of inhibition of eIF4G binding to eIF4E by 4EGI compounds.

Small-molecule inhibitors of the eIF4E/eIF4G interaction provide a novel chemical genetic tool with which to investigate translational control of gene expression. This approach could potentially be used in the study of the many cellular processes, such as cell growth, embryonic development, apoptosis, synaptic plasticity, and axon guidance, in which translational control is involved. Our results also show that antagonists of the eIF4E/eIF4G interaction make up a potential new strategy for small-molecule cancer therapy. Disregulation of a large number of signaling pathways can cause cellular transformation, and many of these pathways converge upon the regulation of cap-dependent translation initiation. It is likely that inhibition of cap-dependent translation will thus have therapeutic value against a wide range of cancer types. Although the compound 4EGI-1 is clearly not in the potency range of a lead drug candidate, it does provide a pharmacophore that can be used to develop inhibitors with higher binding affinity for eIF4E through synthesis of libraries of analogs of this compound and through rational design. The determination of the structure of 4EGI-1 or of a tighter binding analog in complex with eIF4E will facilitate this process. In addition, the assay developed in this study can readily be used to screen more and larger libraries of synthetic compounds and natural products to identify other lead compounds. Such molecules could have higher affinity themselves or, if they are found to bind at a different site than 4EGI compounds, could be linked to this scaffold to generate a tighter binding inhibitor structure.

EXPERIMENTAL PROCEDURES

Protein Cloning, Expression, and Purification

The fusion protein GB1-eIF4E was constructed by cloning the full coding sequence of murine eIF4E into a GB1 expression vector between the BamHI and EcoRI restriction sites. The sequence of murine eIF4E is identical to human eIF4E in the structured portion of the protein with the exception of the substitution of an E for D174, which is a nonconserved residue. Both the tagged and native forms of murine eIF4E were expressed in *Escherichia coli* in LB or isotopically labeled M9 media, then purified by cap-affinity chromatography on m^7GDP or m^7GTP agarose resin. The affinity resin was prepared as previously described (Edery et al., 1988).

FP/FA Assays

The C-terminal fluorescein-labeled peptide has sequence KYTY DELFQLK and was synthesized by Research Genetics. This sequence contains the $Y(X)_4L\Phi$ motif and was optimized for solubility and binding to eIF4E. The unlabeled eIF4GII peptide has the sequence KKQY DREFLLDFQFMPA and was synthesized at the Tufts University Core facility. For the screening assay a solution containing approximately 5 μM eIF4E, 60 nM labeled peptide, 0.05% bovine γ-globulin, and 2 mM DTT in a buffer composed of 50 mM sodium phosphate and 50 mM potassium chloride at pH 6.5 was used. Measurements of FP and FA were made in black 384-well plates (Corning) using an Analyst plate reader (LJL Biosystems). Compounds were transferred to plates using a custom-built Seiko pin-transfer robot at the Institute for Chemistry and Cell Biology at Harvard Medical School. Both GB1-eIF4E and native eIF4E behave identically in this assay. For measurements of FA to be used in curve fitting, the labeled peptide concentration was increased to 1 μM, and γ-globulin was omitted. The curve fitting for estimation of binding constants used a set of equations based on two- and three-state binding models that were derived by Michael Roehrl as previously described (Roehrl et al., 2004).

NMR Spectroscopy

Protein samples for NMR were prepared in a buffer composed of 50 mM sodium phosphate, 50 mM potassium chloride, and 2 mM DTT at pH 6.5. For protein samples of very high concentration (>300 μM) the DTT concentration was 20 mM. In the backbone assignment experiments, the protein was isotopically labeled with ^{15}N, ^{13}C, and 85% or 90% deuterium. The standard three pairs of triple resonance experiments were recorded: HNCA/HN(CO)CA, HNCO/HN(CA)CO, and HNCACB/HN(CO)CACB. The HNCA/HN(CO)CA dataset was recollected using a higher protein concentration and TROSY versions of the pulse sequences in order to obtain data with higher sensitivity. In addition, a ^{15}N-HSQC-NOESY experiment, HSQCs of specific ^{15}N-Lys-, ^{15}N-Ile-, ^{15}N-Leu-, and ^{15}N-Val-labeled samples of

GB1-eIF4E and an HSQC of a reverse-Arg-labeled sample were recorded to facilitate the backbone assignments. For ^{1}H titration experiments of compounds with GB1-eIF4E the compound concentration was 40 μM, and perdeuterated protein was used. For the ^{15}N-HSQC titration the GB1-eIF4E concentration was 25 μM, and the protein was fully protonated. NMR data were processed using NMRPipe (Delaglio et al., 1995), and NMR spectra were analyzed using the software packages XEASY (Bartels et al., 1995) and CARA (which can be downloaded from www.nmr.ch; Keller, 2004).

In Vitro Translation Assays

The dicistronic reporter construct that contains the *Renilla reniformis* luciferase sequence after the 5′ UTR, followed by the CrPV IRES and the firefly luciferase sequence, has been previously described (Wilson et al., 2000) and was generously provided by Tatyana Pestova. The reporter construct plasmid was linearized with BamHI and transcribed in vitro with an ARCA cap using the mMessage Machine T7 Ultra Kit (Ambion). In vitro translation reactions were carried out using Red Nova reticulocyte lysate (Novagen) with 2 mM magnesium acetate and 153 mM potassium acetate, which was incubated at 30°C for 90 min. Translation of reporter genes was measured using the Dual-Glo luciferase assay (Promega) in a Wallac Victor^{2} plate reader. For measurement of translation from the HCV IRES and EMCV IRES, the previously described dicistronic reporter constructs were used (Bordeleau et al., 2006). Uncapped mRNA containing the HCV IRES or EMCV IRES was prepared using the Megascript T3 kit (Ambion), and in vitro translation reactions were run in rabbit reticulocyte lysate as for the CrPV IRES construct.

m^{7}GTP Pull-Down Assay

For the in vitro version of the assay, aliquots of Red Nova reticulocyte lysate with the same salt and buffer concentrations as in the translation reactions were incubated with compound or 200 μM m^{7}GDP for 1 hr at 37°C. Following incubation the lysate was incubated with m^{7}GTP-Sepharose beads (Pharmacia) for 1 hr at 4°C. After washing of the resin, the bound proteins were eluted with free m^{7}GTP, resolved by SDS-PAGE, and analyzed by western blotting using a polyclonal antibody against 4E-BP1 (Cell Signaling Technology) and monoclonal antibodies against eIF4E and eIF4G (Transduction Laboratories). For analysis of binding of purified eIF4E to purified 4E-BP1, the two proteins were mixed (with eIF4E at 920 nM concentration and 4E-BP1 at 770 nM concentration) and subjected to the same protocol as above, with bound eIF4E and 4E-BP1 detected by silver staining using the SilverQuest kit (Invitrogen). Purified 4E-BP1 was obtained from Santa Cruz Biotechnology. For the cell-based version of the assay, Jurkat cells were grown for 6 hr in the presence of the compound, harvested by centrifugation, and lysed by multiple freeze-thaw cycles. Extracts prepared by this method were analyzed using the same pull-down protocol as with the reticulocyte lysates. Phosphorylated forms of 4E-BP1 were detected using polyclonal antibodies (Cell Signaling Technology).

Cell Culture Experiments

For analysis of cellular protein and mRNA levels, Jurkat cells were grown for 8 hr in the presence of the compound. Extracts for protein analysis were prepared from half of the cells by multiple freeze-thaw cycles. The levels of β-actin, Bcl-xL, and c-Myc were analyzed by western blotting using protein-specific polyclonal antibodies (Cell Signaling Technology). The other half of the cells was used for mRNA analysis. The PARIS kit (Ambion) was used to isolate separate fractions of cytosolic and nuclear RNA. As described in the PARIS manual, agarose gel electrophoresis was used to confirm the integrity of the fractionation. Trace DNA was removed from the cytosolic fraction using the DNA-*free* kit (Ambion), and cDNA was prepared using MMLV reverse transcriptase (Promega). Real-time PCR quantitation of c-*myc* and Bcl-xL mRNA relative to β-actin was done using the $\Delta\Delta C_T$ method. Real-time PCR was performed in triplicate with an Applied Biosystems thermocycler using the QuantiTec SYBR Green Kit (Qiagen). Sequence-validated QuantiTec probes (Qiagen) were used for the c-*myc*, the Bcl-xL, and the β-actin mRNAs.

Cell viability was measured by treatment of Jurkat cells with compound for 24 hr and by determination of intracellular ATP using the CellTiterGlo assay (Promega). For measurement of apoptotic DNA fragmentation, cells were treated for 24 hr with 60 μM EGI-1 or 6.65 μM camptothecin in the presence or absence of 100 μM zVAD-FMK, a broad-spectrum caspase inhibitor. After fixation and staining with PI, cellular DNA content was determined by FACS analysis in a FACS-Calibur machine (Beckton Dickinson). Nuclear morphology after 24 hr EG1-1 treatment was visualized by staining of cells with Hoechst 33342 dye and fluorescence microscopy. For the A549 lung cancer cells, cell growth in the presence of 4EGI-1 was determined using the SRB staining method as previously described (Fan et al., 2004).

To determine the selectivity of eIF4E/4G inhibitors for transformed cells, we employed two isogenic cell lines: nontransformed mouse Ba/F3 cells and Ba/F3 cells transformed through transfection with p210 bcr/abl, which were termed Ph^{-} and Ph^{+} cells, respectively (Daley and Baltimore, 1988; both lines were kind gifts from Dr. James Griffin at the Dana Farber Cancer Institute). Cells were cultured in the presence of 5% CO_2 at 37°C in RPMI 1640 medium supplemented with 10% fetal calf serum, WEHI 3B-conditioned medium as a source of IL-3, and penicillin/streptomycin. Cells were plated to 12-well plates at a density of ~10^{5} cells/ml in 2 ml media and were treated in duplicate with increasing concentration of eIF4E/4G inhibitor keeping DMSO concentration constant. On day 3 a 100 μl aliquot was removed from every well, and cell numbers were determined in a Beckman Coulter cell counter.

Supplemental Data

Supplemental Data include one table and five figures and can be found with this article online at http://www.cell.com/cgi/content/full/128/2/257/DC1/.

ACKNOWLEDGMENTS

We would like to thank Rudolf Fluckiger and Mark Fletcher for help in design of the FP assay; Michael Roehrl for advice in FP data analysis; Jim Follen, David Hayes, Katrina Schulberg, Stewart Rudnicki, Carol Chang, and Caroline Shamu of the Harvard Institute for Chemistry and Cell Biology for assistance with screening; Yaqiao Li for assistance with Jurkat cell culture; Fred Harbinski and Amarnath Natarajan for assistance with A549 cell experiments; Sven Hyberts, Mallika Sastry, Hari Arthanari, and Greg Heffron for advice with NMR spectroscopy; Tatyana Pestova for providing the cricket paralysis virus IRES dual-luciferase reporter construct; and Jerry Pelletier for providing the HCV IRES and EMCV IRES dual-luciferase constructs. This work was supported by grants from the National Institutes of Health (GM47467, EB002026, CA68262, CA87427, and CA078411).

Received: April 6, 2006
Revised: September 15, 2006
Accepted: November 23, 2006
Published: January 25, 2007

REFERENCES

Altmann, M., Schmitz, N., Berset, C., and Trachsel, H. (1997). A novel inhibitor of cap-dependent translation initiation in yeast: p20 competes with eIF4G for binding to eIF4E. EMBO J. *16*, 1114–1121.

Arkin, M.R., and Wells, J.A. (2004). Small-molecule inhibitors of protein-protein interactions: progressing towards the dream. Nat. Rev. Drug Discov. *3*, 301–317.

Avdulov, S., Li, S., Michalek, V., Burrichter, D., Peterson, M., Perlman, D.M., Manivel, J.C., Sonenberg, N., Yee, D., Bitterman, P.B., et al. (2004). Activation of translation complex eIF4F is essential for the

genesis and maintenance of the malignant phenotype in human mammary epithelial cells. Cancer Cell *5*, 553–563.

Averous, J., and Proud, C.G. (2006). When translation meets transformation: the mTOR story. Oncogene *25*, 6423–6435.

Bartels, C., Xia, T.H., Billeter, M., Güntert, P., and Wüthrich, K. (1995). The program XEASY for computer-supported NMR spectral analysis of biological macromolecules. J. Biomol. NMR *5*, 1–10.

Bjornsti, M.A., and Houghton, P.J. (2004). The TOR pathway: a target for cancer therapy. Nat. Rev. Cancer *4*, 335–348.

Bordeleau, M.E., Matthews, J., Wojnar, J.M., Lindqvist, L., Novac, O., Jankowsky, E., Sonenberg, N., Northcote, P., Teesdale-Spittle, P., and Pelletier, J. (2005). Stimulation of mammalian translation initiation factor eIF4A activity by a small molecule inhibitor of eukaryotic translation. Proc. Natl. Acad. Sci. USA *102*, 10460–10465.

Bordeleau, M.E., Mori, A., Oberer, M., Lindqvist, L., Chard, L.S., Higa, T., Belsham, G.J., Wagner, G., Tanaka, J., and Pelletier, J. (2006). Functional characterization of IRESes by an inhibitor of the RNA helicase eIF4A. Nat Chem Biol. *2*, 213–220.

Daley, G.Q., and Baltimore, D. (1988). Transformation of an interleukin 3-dependent hematopoietic cell line by the chronic myelogenous leukemia-specific P210bcr/abl protein. Proc. Natl. Acad. Sci. USA *85*, 9312–9316.

De Benedetti, A., and Graff, J.R. (2004). eIF-4E expression and its role in malignancies and metastases. Oncogene *23*, 3189–3199.

DeFatta, R.J., Nathan, C.A., and De Benedetti, A. (2000). Antisense RNA to eIF4E suppresses oncogenic properties of a head and neck squamous cell carcinoma cell line. Laryngoscope *110*, 928–933.

Delaglio, F., Grzesiek, S., Vuister, G., Zhu, G., Pfeifer, J., and Bax, A. (1995). NMRPipe: a multidimensional spectral processing system based on UNIX pipes. J. Biomol. NMR *6*, 277–293.

Dever, T.E. (2002). Gene-specific regulation by general translation factors. Cell *108*, 545–556.

Edery, I., Altmann, M., and Sonenberg, N. (1988). High-level synthesis in Escherichia coli of functional cap-binding eukaryotic initiation factor eIF-4E and affinity purification using a simplified cap-analog resin. Gene *74*, 517–525.

Faivre, S., Kroemer, G., and Raymond, E. (2006). Current development of mTOR inhibitors as anticancer agents. Nat. Rev. Drug Discov. *5*, 671–688.

Fan, Y.H., Chen, H., Natarajan, A., Guo, Y., Harbinski, F., Iyasere, J., Christ, W., Aktas, H., and Halperin, J.A. (2004). Structure-activity requirements for the antiproliferative effect of troglitazone derivatives mediated by depletion of intracellular calcium. Bioorg. Med. Chem. Lett. *14*, 2547–2550.

Fukuchi-Shimogori, T., Ishii, I., Kashiwagi, K., Mashiba, H., Ekimoto, H., and Igarashi, K. (1997). Malignant transformation by overproduction of translation initiation factor eIF4G. Cancer Res. *57*, 5041–5044.

Gingras, A.C., Raught, B., and Sonenberg, N. (1999). eIF4 initiation factors: effectors of mRNA recruitment to ribosomes and regulators of translation. Annu. Rev. Biochem. *68*, 913–963.

Gingras, A.C., Raught, B., Gygi, S.P., Niedzwiecka, A., Miron, M., Burley, S.K., Polakiewicz, R.D., Wyslouch-Cieszynska, A., Aebersold, R., and Sonenberg, N. (2001). Hierarchical phosphorylation of the translation inhibitor 4E–BP1. Genes Dev. *15*, 2852–2864.

Gross, J.D., Moerke, N.J., von der Haar, T., Lugovskoy, A.A., Sachs, A.B., McCarthy, J.E., and Wagner, G. (2003). Ribosome loading onto the mRNA cap is driven by conformational coupling between eIF4G and eIF4E. Cell *115*, 739–750.

Haghighat, A., Mader, S., Pause, A., and Sonenberg, N. (1995). Repression of cap-dependent translation by 4E-binding protein 1: competition with p220 for binding to eukaryotic initiation factor-4E. EMBO J. *14*, 5701–5709.

Herbert, T.P., Fahraeus, R., Prescott, A., Lane, D.P., and Proud, C.G. (2000). Rapid induction of apoptosis mediated by peptides that bind initiation factor eIF4E. Curr. Biol. *10*, 793–796.

Hershey, J.W.B., and Merrick, W.C. (2000). The pathway and mechanism of initiation of protein synthesis. In Translational Control of Gene Expression, N. Sonenberg, J.W.B. Hershey, and M.B. Mathews, eds. (Cold Spring Harbor, NY: Cold Spring Harbor Laboratory Press), pp. 33–88.

Hershey, P.E., McWhirter, S.M., Gross, J.D., Wagner, G., Alber, T., and Sachs, A.B. (1999). The Cap-binding protein eIF4E promotes folding of a functional domain of yeast translation initiation factor eIF4G1. J. Biol. Chem. *274*, 21297–21304.

Huang, S., and Houghton, P.J. (2003). Targeting mTOR signaling for cancer therapy. Curr. Opin. Pharmacol. *3*, 371–377.

Inoki, K., Corradetti, M.N., and Guan, K.L. (2005). Dysregulation of the TSC-mTOR pathway in human disease. Nat. Genet. *37*, 19–24.

Keller, R. (2004). The Computer Aided Resonance Assignment Tutorial, First Edition (Goldau, Switzerland: Cantina Verlag).

Koradi, R., Billeter, M., and Wuthrich, K. (1996). MOLMOL: a program for display and analysis of macromolecular structures. J Mol Graph. *14*, 51–55, 29–32.

Koromilas, A.E., Lazaris-Karatzas, A., and Sonenberg, N. (1992). mRNAs containing extensive secondary structure in their 5′ noncoding region translate efficiently in cells overexpressing initiation factor eIF-4E. EMBO J. *11*, 4153–4158.

Lazaris-Karatzas, A., Montine, K.S., and Sonenberg, N. (1990). Malignant transformation by a eukaryotic initiation factor subunit that binds to mRNA 5′ cap. Nature *345*, 544–547.

Lee, C.H., Inoki, K., and Guan, K.L. (2006). mTOR pathway as a target in tissue hypertrophy. Annu Rev Pharmacol Toxicol., in press. Published online January 20, 2006. 10.1146/annurev.pharmtox.47.120505.105359.

Li, S., Sonenberg, N., Gingras, A.C., Peterson, M., Avdulov, S., Polunovsky, V.A., and Bitterman, P.B. (2002). Translational control of cell fate: availability of phosphorylation sites on translational repressor 4E–BP1 governs its proapoptotic potency. Mol. Cell. Biol. *22*, 2853–2861.

Lodish, H.F. (1976). Translational control of protein synthesis. Annu. Rev. Biochem. *45*, 39–72.

Mader, S., Lee, H., Pause, A., and Sonenberg, N. (1995). The translation initiation factor eIF-4E binds to a common motif shared by the translation factor eIF-4 gamma and the translational repressors 4E-binding proteins. Mol. Cell. Biol. *15*, 4990–4997.

Mamane, Y., Petroulakis, E., LeBacquer, O., and Sonenberg, N. (2006). mTOR, translation initiation and cancer. Oncogene *25*, 6416–6422.

Marcotrigiano, J., Gingras, A.C., Sonenberg, N., and Burley, S.K. (1999). Cap-dependent translation initiation in eukaryotes is regulated by a molecular mimic of eIF4G. Mol. Cell *3*, 707–716.

Matsuo, H., Li, H., McGuire, A.M., Fletcher, C.M., Gingras, A.C., Sonenberg, N., and Wagner, G. (1997). Structure of translation factor eIF4E bound to m7GDP and interaction with 4E-binding protein. Nat. Struct. Biol. *4*, 717–724.

Miura, T., Shiratori, Y., and Shimma, N. (2003). Backbone resonance assignment of human eukaryotic translation initiation factor 4E (eIF4E) in complex with 7-methylguanosine diphosphate (m7GDP) and a 17-amino acid peptide derived from human eIF4GII. J. Biomol. NMR *27*, 279–280.

Novac, O., Guenier, A.S., and Pelletier, J. (2004). Inhibitors of protein synthesis identified by a high throughput multiplexed translation screen. Nucleic Acids Res. *32*, 902–915.

Pause, A., Belsham, G.J., Gingras, A.C., Donze, O., Lin, T.A., Lawrence, J.C., Jr., and Sonenberg, N. (1994). Insulin-dependent

stimulation of protein synthesis by phosphorylation of a regulator of 5′-cap function. Nature *371*, 762–767.

Pestova, T.V., and Hellen, C.U. (2003). Translation elongation after assembly of ribosomes on the Cricket paralysis virus internal ribosomal entry site without initiation factors or initiator tRNA. Genes Dev. *17*, 181–186.

Petroulakis, E., Mamane, Y., Le Bacquer, O., Shahbazian, D., and Sonenberg, N. (2006). mTOR signaling: implications for cancer and anticancer therapy. Br. J. Cancer *94*, 195–199.

Pickering, B.M., and Willis, A.E. (2005). The implications of structured 5′ untranslated regions on translation and disease. Semin. Cell Dev. Biol. *16*, 39–47.

Polunovsky, V.A., Gingras, A.C., Sonenberg, N., Peterson, M., Tan, A., Rubins, J.B., Manivel, J.C., and Bitterman, P.B. (2000). Translational control of the antiapoptotic function of Ras. J. Biol. Chem. *275*, 24776–24780.

Richter, J.D., and Sonenberg, N. (2005). Regulation of cap-dependent translation by eIF4E inhibitory proteins. Nature *433*, 477–480.

Roehrl, M.H., Wang, J.Y., and Wagner, G. (2004). A general framework for development and data analysis of competitive high-throughput screens for small-molecule inhibitors of protein-protein interactions by fluorescence polarization. Biochemistry *43*, 16056–16066.

Rousseau, D., Gingras, A.C., Pause, A., and Sonenberg, N. (1996). The eIF4E-binding proteins 1 and 2 are negative regulators of cell growth. Oncogene *13*, 2415–2420.

Ruggero, D., and Pandolfi, P.P. (2003). Does the ribosome translate cancer? Nat. Rev. Cancer *3*, 179–192.

Ruggero, D., Montanaro, L., Ma, L., Xu, W., Londei, P., Cordon-Cardo, C., and Pandolfi, P.P. (2004). The translation factor eIF-4E promotes tumor formation and cooperates with c-Myc in lymphomagenesis. Nat. Med. *10*, 484–486.

Sawyers, C.L. (2003). Will mTOR inhibitors make it as cancer drugs? Cancer Cell *4*, 343–348.

Svitkin, Y.V., Pause, A., Haghighat, A., Pyronnet, S., Witherell, G., Belsham, G.J., and Sonenberg, N. (2001). The requirement for eukaryotic initiation factor 4A (eIF4A) in translation is in direct proportion to the degree of mRNA 5′ secondary structure. RNA *7*, 382–394.

Tee, A.R., and Blenis, J. (2005). mTOR, translational control and human disease. Semin. Cell Dev. Biol. *16*, 29–37.

Tomoo, K., Abiko, F., Miyagawa, H., Kitamura, K., and Ishida, T. (2006). Effect of N-terminal region of eIF4E and Ser65-phosphorylation of 4E–BP1 on interaction between eIF4E and 4E–BP1 fragment peptide. J Biochem (Tokyo). *140*, 237–246.

von der Haar, T., Gross, J.D., Wagner, G., and McCarthy, J.E. (2004). The mRNA cap-binding protein eIF4E in post-transcriptional gene expression. Nat. Struct. Mol. Biol. *11*, 503–511.

Wendel, H.G., De Stanchina, E., Fridman, J.S., Malina, A., Ray, S., Kogan, S., Cordon-Cardo, C., Pelletier, J., and Lowe, S.W. (2004). Survival signalling by Akt and eIF4E in oncogenesis and cancer therapy. Nature *428*, 332–337.

Wilson, J.E., Powell, M.J., Hoover, S.E., and Sarnow, P. (2000). Naturally occurring dicistronic cricket paralysis virus RNA is regulated by two internal ribosome entry sites. Mol. Cell. Biol. *20*, 4990–4999.

Wullschleger, S., Loewith, R., and Hall, M.N. (2006). TOR signaling in growth and metabolism. Cell *124*, 471–484.

Zhou, P., Lugovskoy, A.A., and Wagner, G. (2001). A solubility-enhancement tag (SET) for NMR studies of poorly behaving proteins. J. Biomol. NMR *20*, 11–14.